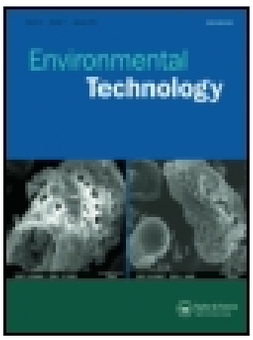

Environmental Technology

ISSN: 0959-3330 (Print) 1479-487X (Online) Journal homepage: http://www.tandfonline.com/loi/tent20

Treatment of aqueous solutions of 1,4-dioxane by ozonation and catalytic ozonation with copper oxide (CuO)

Gidiane Scaratti, Alex Basso, Richard Landers, Pedro J. J. Alvarez, Gianluca Li Puma & Regina F. P. M. Moreira

To cite this article: Gidiane Scaratti, Alex Basso, Richard Landers, Pedro J. J. Alvarez, Gianluca Li Puma & Regina F. P. M. Moreira (2018): Treatment of aqueous solutions of 1,4-dioxane by ozonation and catalytic ozonation with copper oxide (CuO), Environmental Technology, DOI: 10.1080/09593330.2018.1538259

To link to this article: https://doi.org/10.1080/09593330.2018.1538259

Accepted author version posted online: 19 Oct 2018.
Published online: 29 Oct 2018.

ENVIRONMENTAL TECHNOLOGY
https://doi.org/10.1080/09593330.2018.1538259

Taylor & Francis
Taylor & Francis Group

Treatment of aqueous solutions of 1,4-dioxane by ozonation and catalytic ozonation with copper oxide (CuO)

Gidiane Scaratti [a], Alex Basso[a], Richard Landers[b], Pedro J. J. Alvarez[c], Gianluca Li Puma[d] and Regina F. P. M. Moreira [a]

[a]Department of Chemical and Food Engineering, Federal University of Santa Catarina, Florianópolis, SC, Brazil; [b]Institute of Physics Gleb Wataghin, University of Campinas, Campinas, SP, Brazil; [c]Department of Civil and Environmental Engineering, Rice University, Houston, TX, USA; [d]Environmental Nanocatalysis & Photoreaction Engineering, Department of Chemical Engineering, Loughborough University, Loughborough, UK

ABSTRACT

In this study, treatment for the removal of 1,4-dioxane by ozone and by catalytic ozonation using CuO as the catalyst was investigated. While the removal of 1,4-dioxane was small (20%) and mineralization negligible after 6 h of ozonation treatment, the removals of 1,4-dioxane and total organic carbon increased by factors of 10.35 and 81.25, respectively, after catalytic ozonation in the presence of CuO. The mineralization during catalytic ozonation was favoured at pH 10 (94.91 min^{-1}), although it proceeded even at pH 3 (54.41 min^{-1}). The CuO catalyst decreased the equilibrium concentration of soluble ozone and favoured its decomposition to reactive oxidative species. Radical scavenging experiments demonstrated that superoxide radicals were the main species responsible for the degradation of 1,4-dioxane. Further scavenging experiments with phosphate confirmed the presence of Lewis active sites on the surface of CuO, which were responsible for the adsorption and decomposition of ozone. The reaction mechanism proceeded through the formation of ethylene glycol diformate, which quickly hydrolyzed to ethylene glycol and formic acid as intermediate products. The stability of CuO indicated weak copper leaching and high catalytic activity for five recycling cycles. The toxicity of the water, assessed by *Vibrio fischeri* bioluminescence assays, remained the same (low toxicity) after catalytic ozonation while it increased after treatment with ozonation alone.

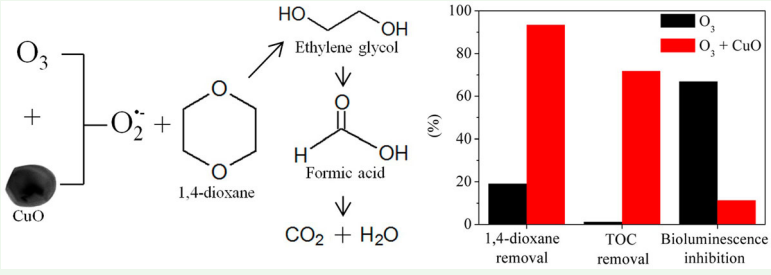

ARTICLE HISTORY
Received 18 July 2018
Accepted 12 October 2018

KEYWORDS
1,4-dioxane; groundwater contamination; catalytic ozonation; copper oxide; advanced oxidation processes

Highlights

- 1,4-Dioxane can be totally removed applying catalytic ozonation with CuO
- Superoxide radicals were responsible for 1,4-dioxane removal
- Major reaction intermediates of 1,4-dioxane were identified
- Acute toxicity during catalytic ozonation is low

Introduction

1,4-dioxane is a synthetic cyclic ether traditionally used as a chlorinated solvent stabilizer. It is a contaminant often detected in groundwater or at sites contaminated with 1,1,1-trichloroethane or trichloroethene. 1,4-Dioxane has been detected in municipal water supply wells [1] and river, ocean and groundwater samples [2] in concentrations in the range of 1.9 to 2100 ppb. These contaminated sites are typically in locations

CONTACT Gidiane Scaratti gidiane@gmail.com Department of Chemical and Food Engineering, Federal University of Santa Catarina, Laboratory of Energy and Environmental, CEP: 880410-900, Florianópolis, SC, Brazil

where degreasing operations associated with military equipment or electronic components have taken place, or near dry cleaners and industrial complexes. 1,4-Dioxane is also a common by-product of chemical processes involving the production or use of ethylene glycol [3,4] and, as a result, can also be present in industrial wastewaters, some of them with high 1,4-dioxane concentrations of around 250 ppm [5].

Concern regarding the impact of 1,4-dioxane on the environment has increased in recent years, particularly since this compound has been classified as a priority hazardous pollutant and a probable human carcinogen [6,7]. 1,4-Dioxane has a high aqueous solubility, low vapour pressure and a boiling point similar to that of water [3,4,8,9]. It is a relatively bio-recalcitrant and persistent organic molecule that is resilient to treatment by conventional processes, such as adsorption onto activated carbon or air stripping. Consequently, advanced treatment processes for the degradation of 1,4-dioxane in contaminated groundwater have been investigated, including biodegradation [10], chemical oxidation by Fenton and hydrogen peroxide/UV processes [11,12], ozone (O_3) with hydrogen peroxide, persulfate and peroxone-activated persulfate [13–15]. When O_3 is used as the sole oxidant it has been found to be relatively ineffective, since the 1,4-dioxane molecule does not present reacting sites that favour direct attack by O_3 [13,16–19]. However, under basic conditions, ozonation was found to be a more attractive technology in terms of operating cost and COD reduction when compared with heterogeneous Fe^0-based photo-Fenton and conductive diamond electrochemical oxidation for the pretreatment of 1,4-dioxane-containing wastewater from a chemical manufacturing industry [5].

Catalytic ozonation is an effective advanced oxidation process (AOP) for the removal of organic contaminants from water and wastewater [20–23], owing to its ability to decompose the ozone molecule to highly reactive radical species, which rapidly react with organic contaminants. Several solid catalysts, such as iron oxides [20,24–26], ceria oxide [27,28], activated carbon [29,30] and Fe^0 [31], have been used successfully to catalyze the decomposition of organic compounds in wastewaters using ozone or hydrogen peroxide. In general, the catalytic activity is related to the BET surface area, crystallinity and ability to produce free radicals from ozone or hydrogen peroxide [32]. In addition, catalytic ozonation generally has a low impact on the water quality after treatment and is a process that is easy to implement at the industrial scale at a relatively low cost [33]. The catalytic ozonation of water contaminated with 1,4-dioxane has been reported in only one study, employing activated carbon as the catalyst (efficiency of 1,4-dioxane removal was 95% for 3000 ppm of activated carbon) [29], and the use of metal oxides as catalysts has not been reported.

With regard to metal oxides, copper oxide (CuO) has often been used as an effective ozonation catalyst, since it offers good catalytic properties, favouring a high density of adsorbed hydroxyl groups on the surface, which significantly enhances the decomposition of ozone and the degradation of aqueous organic pollutants [21,34]. In addition, CuO is inexpensive, chemically stable and presents much lower toxicity in relation to other ozone-activating catalysts [34].

The catalytic mechanism of action of CuO toward ozone and in the oxidation of organic compounds remains controversial, particularly since the oxidation can follow a hydroxyl radical or a non-hydroxyl radical oxidation pathway [27]. In general, hydroxyl radicals (•OH) react quickly and non-selectively with a large number of organic compounds in water, while O_3 reacts quickly with unsaturated organic compounds and slowly with saturated ones [32]. However, hydroxyl radicals can also react with ozone ($k_{\cdot OH} = 1 \times 10^8 - 2 \times 10^9\ M^{-1}\ s^{-1}$) and bicarbonate/carbonate ($k_{\cdot OH} = 8.5 \times 10^6/3.9 \times 10^8\ M^{-1}\ s^{-1}$) [28]. Thus, it is expected that the •OH reaction with saturated hydrophilic organic species and by-products in the presence of ozone is relatively slow due to the competitive reaction of •OH and ozone [35].

In this study, the effectiveness of CuO as catalyst for the decomposition of ozone and degradation of aqueous solutions of 1,4-dioxane through catalytic ozonation was investigated. The morphological, physical, chemical and catalytic properties of the CuO catalyst were determined using several analytical techniques, including transmission electron microscopy (TEM), X-ray diffraction (XRD), surface area and porosity analysis (BET-BJS), atomic absorption spectrometry (AAS), zeta-potential measurements, Fourier transform infrared spectroscopy (FTIR) and X-ray photoelectron spectroscopy (XPS). The degradation kinetics of 1,4-dioxane, as a function of the pH and catalyst dosage, was assessed in terms of total organic carbon (TOC) and 1,4-dioxane removal, and the underlying mechanisms of ozonation and catalytic ozonation, the stability and the reusability of the catalyst were investigated. The acute toxicity toward *Vibrio fischeri* of the water before and after treatment with ozonation and with catalytic ozonation was evaluated to determine the efficiency of the treatment processes for practical water remediation.

Material and methods

Chemicals and materials

All reagents used were analytical grade and solutions were prepared with deionized water. 1,4-Dioxane (99.99%) was

supplied by Neon (Brazil). Commercial copper oxide (99% of purity) was purchased from Amorphous and Nanostructures Materials Inc. (Houston, TX, USA). Sodium dihydrogen phosphate (NaH_2PO_4) was purchased from Vetec (Brazil), 1,4-benzoquinone ($C_6H_4O_2$) from Sigma Aldrich (USA), salicylic acid ($C_7H_6O_3$) from Reagen (Brazil) and sodium fluoride (NaF) from Synth (Brazil).

Characterization of the catalyst

The morphology of the CuO particles was determined by transmission electron microscopy (TEM) (JEOL, JEM-1011). The crystalline phases in the samples were determined by X-ray diffraction (XRD) on a Bruker D2-Phaser diffractometer with CuKα radiation ($\lambda = 1.54056$ Å), from 10° to 70°.

The specific surface area (S_{BET}) and pore diameter distribution of the CuO, according to the Barret-Joyner-Halenda (BJH) method, were determined by N_2 adsorption-desorption experiments. Analysis was carried out by means of isotherms obtained on an Autosorb 1C (Quantachrome, USA) adsorptometer. Prior to the analysis, the samples were degassed for 12 h at 140°C under vacuum.

The zeta potential (ξ) of aqueous suspensions of CuO (0.5 g of CuO in 50 mL of deionized water) as a function of pH (from 3 to 10) was measured using a Stabino NANO-flex particle. The zeta potential was determined from the electrophoretic mobility (μ) based on the Smoluchowski equation. NaOH and HCl (0.01 N solutions) were used as titration media to automatically adjust the pH values.

The Cu content of the catalysts was determined using atomic absorption spectroscopy (AAS). In this procedure, 1.0 mg of the catalyst was solubilized in 20 mL of concentrated HNO_3 and HCl solution and evaporated to less than 5 mL [36]. After solubilization, the samples were transferred to volumetric flasks. The volume was adjusted to 50 mL with distilled water and analyzed via AAS with an Agilent 240FSAA spectrometer.

Fourier transform infrared (FTIR) spectra of CuO before use and after 5 treatment cycles were recorded between 400 and 4000 cm^{-1} using an FTIR spectrometer (Agilent Technologies – Cary 600 Series).

The X-ray photoelectron spectroscopy (XPS) spectra were obtained with a VSW HA-100 spherical analyzer and MgKα radiation (hv = 1253.6 eV). The high-resolution spectra were measured with constant analyzer pass energies of 44 eV. The pressure during the measurements was always less than 2×10^{-8} mbar. The sample was fixed to a stainless steel sample holder with double-faced conducting tape and analyzed without further preparation. Surface charge was corrected, shifting all spectra so that the C1s line associated with adventitious carbon was at 284.6 eV. Curve fitting was performed using Gaussian line shapes and a Shirley background was subtracted from the data.

Ozonation and catalytic ozonation experiments

Ozonation experiments were carried out isothermally at 25°C in a 1.5 L glass-jacketed vessel (21 cm height and 8 cm diameter) continuously stirred (~500 rpm) with a magnetic stirrer (Dist – model DI-03). In a typical procedure, 1.5 L of a 200 ppm 1,4-dioxane aqueous solution was transferred into the reactor, the pH was adjusted to the desired level using 0.5 M H_2SO_4 or 0.5 M NaOH solutions, and a specific catalyst dose (when used) was added. Ozone was then continuously bubbled into the vessel through two air diffusers at a rate of 0.063 $m^3\ h^{-1}$. The reactor was operated in semi-batch mode for 6 h. Samples withdrawn at regular intervals were filtered through a PVDF membrane (Millipore; 0.22 µm pore size) for the analytical determination of the TOC, 1,4-dioxane concentration [1,4-dioxane], aqueous ozone concentration [O_3], pH and acute toxicity.

In previous tests performed to select a suitable catalyst, involving a comparison of the TOC removal and ozone decomposition rate obtained using different non-noble metals (goethite, cerium oxide or copper oxide), copper oxide resulted in the highest catalytic activity [28,37].

Ozone decomposition experiments

The same reactor described above was used to determine the rate of ozone decomposition. The experiments were carried out using 1.5 L of deionized water in the absence of catalyst and in the presence of the CuO catalyst at 0.1, 0.25 or 0.5 ppm. Ozone was then continuously bubbled into the reactor at a rate of 0.063 $m^3\ h^{-1}$, at 25 ± 1°C and at pH 10, 7.0, 5.5 or 3.0. Samples collected at appropriate intervals over a period of 40 min were rapidly filtered through a PVDF membrane (Millipore; 0.22 µm pore size). The residual aqueous ozone concentration (C) was evaluated in a spectrophotometer (HACH DR 5000) by quantifying the absorbance at 258 nm by the Lambert-Beer law (Equation 1).

$$\mathrm{ABS} = \varepsilon L C \tag{1}$$

where ε is the molar extinction coefficient equal to 2950 $M^{-1}\ cm^{-1}$ at 258 nm [36], L is the optical path and C is the ozone concentration in the aqueous phase.

The theoretical aqueous ozone concentration was calculated through the liquid phase mass balance

(Equation 2):

$$\frac{dC_{O_3}}{dt} = k_{La}(C_{sat} - C_{O_3}) - k_T C_{O_3} \quad (2)$$

$$k_T = k_d + wk_{het} \quad (3)$$

where C_{sat} is the saturated ozone concentration, C_{O_3} the aqueous ozone concentration, k_L the volumetric mass transfer coefficient, k_T the ozone decomposition rate constant, k_d the ozone self-decomposition constant, w the catalyst dosage and k_{het} the catalytic ozone decomposition constant. The right-hand side of Equation (2) reduces to a pseudo-first-order rate law under an excess of ozone in the reactor.

The ozone self-decomposition constant (k_d) was obtained through the correlation proposed by Sullivan [38] (Equation 4).

$$k_d = 9.811 \cdot 10^7 [OH^-]^{0.123} \exp\left(\frac{-5606}{T}\right) \quad (4)$$

where $[OH^-]$ is the OH^- concentration and T is the temperature in Kelvin.

Catalyst reuse

The catalyst was reused in selected experiments to assess its stability over multiple cycles. At the end of each cycle, the catalyst was separated by membrane filtration (Millipore; 0.22 µm pore size). The solids were dried at 60 ± 1°C for 15 h and reused for the subsequent cycle without any further purification.

Analytical methods

The pH was determined by the potentiometric method using a pH metre (Quimis, Model Q400A), previously calibrated with pH 4.0 and 7.0 buffer solutions. The concentration of leached copper ion in the liquid phase after the heterogeneous catalytic ozonation reactions was measured using AAS.

The aqueous ozone concentration during the experiments was analyzed as described in section 2.4 and the TOC was determined on a TOC-V_{CPH} analyzer (Shimadzu).

The 1,4-dioxane was extracted according to the methodology proposed by Li and collaborators [39] and quantified using a CG-MS instrument (Shimadzu QP2010 plus) equipped with a Supel-Q PLOT column. The column temperature was maintained at 150°C during the analysis (total time was 4 min) and the injector and interface temperature was 200°C. Samples (1 µL) were injected in split mode (1:18). Helium was used as the carrier gas. The quantification and confirmation ions were *m/z* 88 and *m/z* 58, respectively.

The 1,4-dioxane and TOC degradation rate constants (k_1) were obtained according to the pseudo-first-order rate laws (Equation 5) together with the material balance of the batch reactor, which was operated under an excess of ozone (continuous bubbling).

$$-\ln\left(\frac{C}{C_0}\right) = k_1 t \quad (5)$$

where C_0 and C are the initial concentration and the concentration after the catalytic ozonation process at various time intervals, respectively, k_1 is either the 1,4-dioxane or TOC degradation pseudo-first-order rate constant (min^{-1}) and t is the reaction time. The first-order rate constant (k_1) was determined by the slope of the straight line fitting of $-\ln(C/C_0)$ versus time.

The acute toxicity test with the bioluminescent bacteria *Vibrio fischeri* (lyophilized) was performed according to the methodology proposed by ISO 11348-3 [40].

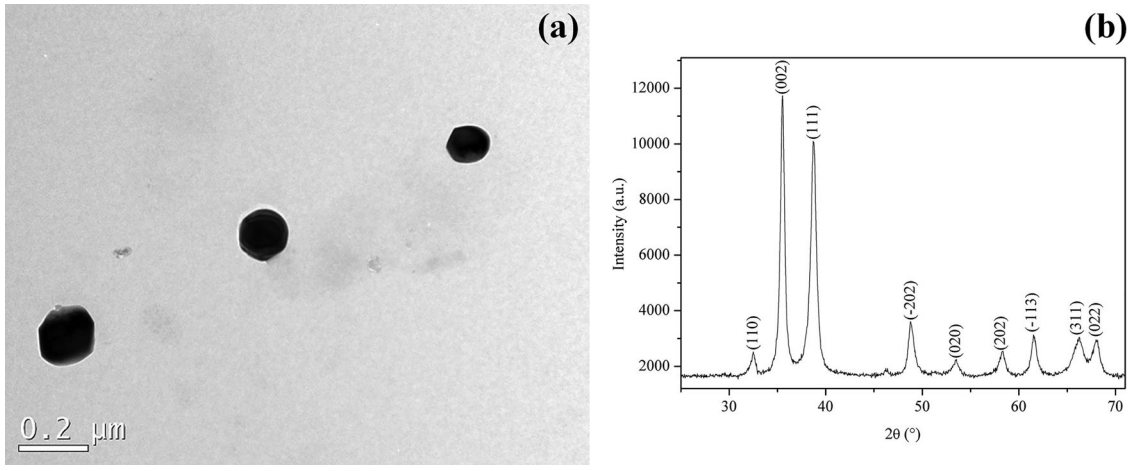

Figure 1. (a) TEM images of CuO and (b) XRD of CuO.

Table 1. Characterization of CuO particles.

Particle Size, nm	77–200
Purity, %	100%
Point of zero charge	7.41
BET surface area, m^2/g	12.61
Pore size diameter, nm	3.6 nm
Total pore volume, $cm^3\ g^{-1}$	0.044

Results and discussion

Catalyst characterization

The morphology of the CuO powder is shown in the TEM images in Figure 1. The CuO particles had irregular spherical shapes with different diameters and were well distributed without aggregation [41,42]. The XRD pattern for CuO, with lattice planes of vibration, can be seen in Figure 1b (JCPDS 48-1548). The XRD analysis showed a series of diffraction peaks at $2\theta = 32.4°$, 35.6°, 38.8°, 48.9°, 53.3°, 58.2°, 61.6°, 66.3° and 67.9° characteristic of the monoclinic phase of copper (II) oxide [43].

The results for the main parameters used to characterize the CuO particles are shown in Table 1. High purity and low surface area are notable features of the catalyst used in this study.

The oxidation state of the CuO before and after the catalytic ozonation of 1,4-dioxane was investigated by XPS (Figure 2). The O1s spectra for the CuO after and before catalytic ozonation can be seen in Figure 2a and b, respectively. The peaks at 528.97–529.21 eV were attributed to lattice oxygen and the peaks at 530.76–531.10 eV were assigned to O-C, as well as to the oxygen adsorbed at the surface [44,45]. The smallest peak, observed only for the sample before catalytic ozonation at 533.17 eV, was assigned to O-H and/or to oxygen adsorbed at the surface [44,46].

Figure 2c and d show the two doublets Cu-$2p_{3/2}$ and Cu-$2p_{1/2}$, presenting energetic differences of 20 eV, in good agreement with data published in the literature [46]. In general, copper oxide can exist in two phases,

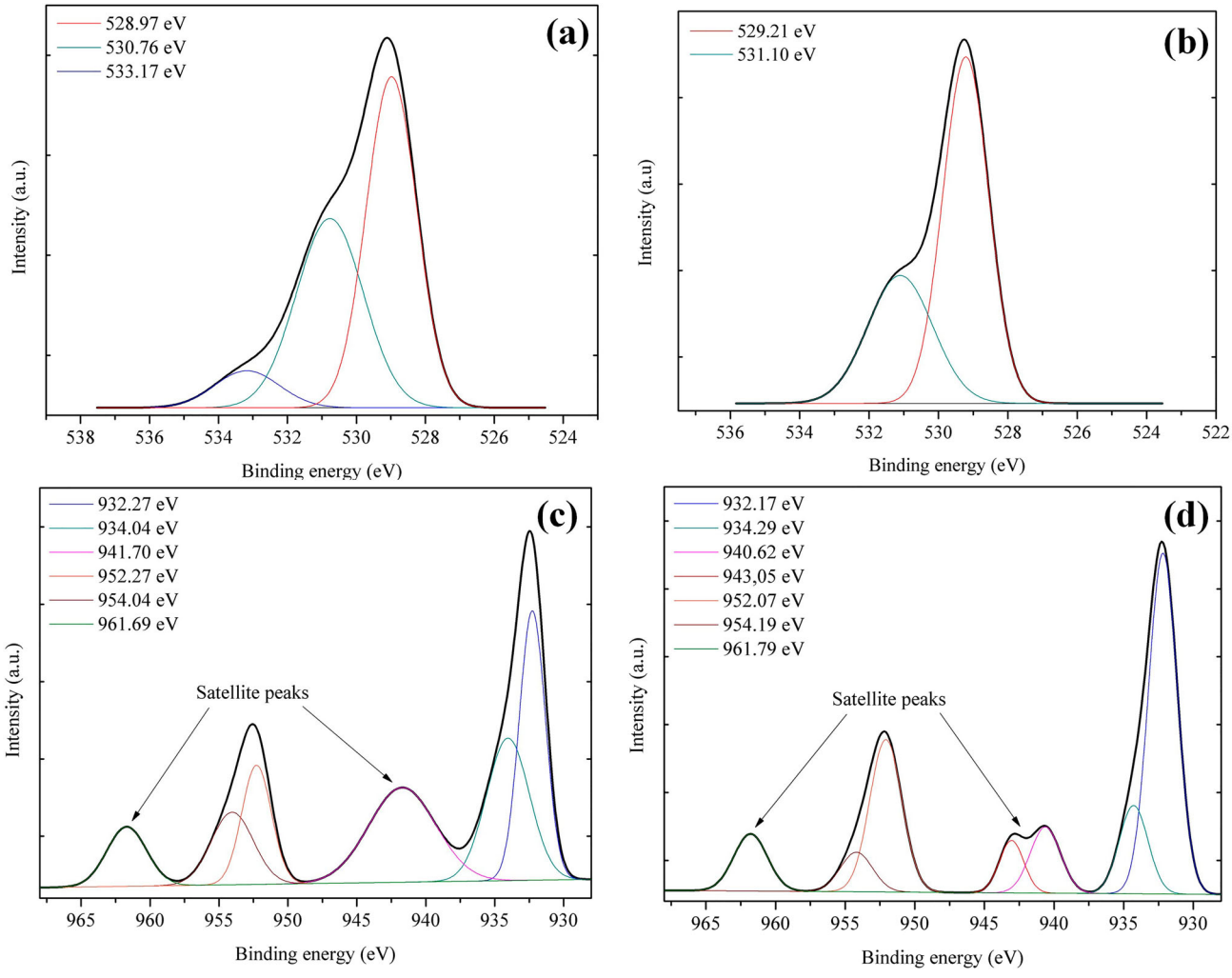

Figure 2. XPS spectra: (a, c) CuO before catalytic ozonation and (b, d) CuO after catalytic ozonation (ozone flow = 0.064 $m^3\ h^{-1}$; $T = 25 \pm 1$°C).

cupric oxide (CuO) and cuprous oxide (Cu_2O). The peaks at 934.2 and 954.2 eV are attributed to CuO (Cu^{2+}). However, the peaks at 932.2 and 952.2 eV are attributed to Cu_2O (Cu^{+}), indicating the presence of Cu_2O on the solid surface of the sample caused by redox reactions on the solid surface [47]. The satellite peaks in the spectra (941.7, 943.05 and 961.7 eV) are associated with the presence of Cu(II) (CuO) [45,46]. Since no Cu_2O diffractions peaks were detected in the XRD pattern (Figure 1b), this is restricted to the surface.

For the CuO sample after catalytic ozonation the peaks at 934.2 and 954.2 eV shifted to lower binding energy when compared to the sample before the reaction, which means that more Cu^{+} was present on the CuO surface after ozonation.

Catalytic decomposition of ozone

The impact of CuO on the absorption and decomposition of ozone was determined at different pH values and using different catalyst dosages at pH 5.5 (Figure S1). Table 2 shows the k_d, C_e and k_{het} values, determined by fitting Equation (2) to the experimental results. The values of k_{La} (0.475 ± 0.036 min^{-1}) and C_{sat} (10.264 ± 1.063 ppm) were constant and dependent only on the reaction temperature (25°C) and the mixing conditions in the reactor. The residual concentration of ozone at equilibrium (C_e) showed a small decrease as the pH increased, in the absence of catalyst, since ozone was continuously supplied into the system. In contrast, the ozone decomposition constant (k_d) rapidly increased above pH 7 due to the decomposition of O_3 molecules to •OH radicals [48]. The catalytic ozone decomposition constant (k_{het}) decreased slightly as the catalyst dose was increased, remaining close to the average value of 1.268 ± 0.018. The mechanism of heterogeneous catalytic ozone decomposition, as proposed by Beltrán et al. [48], is described in Equations (6)–(9).

$$OH^- + S \leftrightarrow OH{\bullet}S \quad (6)$$

$$O_3 + OH{\bullet}S \leftrightarrow {\bullet}O_3{\bullet}S + HO{\bullet} \quad (7)$$

$$ {\bullet}O_3{\bullet}S \leftrightarrow {\bullet}O{\bullet}S + O_2 \quad (8)$$

$$O_3 + {\bullet}O{\bullet}S \leftrightarrow O_2{\bullet} + S + O_2 \quad (9)$$

where S is the catalyst surface. The above reactions are the steps involved in the surface chemical reaction involving adsorption, surface reaction and desorption processes.

Table 2. The k_d, C_e and k_{het} values for deionized water ozonation at different pH values and catalyst dosages ($k_{La} = 0.475 \pm 0.036$ min^{-1} and $C_{sat} = 10.264 \pm 1.063$ ppm) (ozone flow rate = 0.064 m^3 h^{-1}; $T = 25 \pm 1$°C).

CuO dosage/pH	k_d (min^{-1})	C_e (ppm)	k_{het} (min^{-1})
0 ppm/10.0	0.21	7.87 ± 0.03	–
0 ppm/7.0	0.09	8.18 ± 0.16	–
0 ppm/5.5	0.06	8.75 ± 0.06	–
0 ppm/3.0	0.03	9.16 ± 0.17	–
0.1 ppm/5.5	0.06	4.31 ± 0.01	1.34 ± 0.01
0.25 ppm/5.5	0.06	4.21 ± 0.01	1.26 ± 0.02
0.5 ppm/5.5	0.06	4.02 ± 0.01	1.20 ± 0.02

Degradation and mineralization of 1,4-dioxane by ozone in the absence of catalyst

The chromatographic analysis showed that 1,4-dioxane could be efficiently removed from the water with ozone alone under alkaline conditions (Figure 3). In contrast, at pH ≤ 7 the rate of degradation was very low. No mineralization was observed under acidic or basic pH, since the pH rapidly decreased during the reaction (Figure S2).

Lower pH values do not favour the decomposition of O_3 to •OH, which has a much greater reactivity with 1,4-dioxane than O_3 [17,19]. This chain mechanism of •OH production is initiated by hydroxide anions at higher pH values, where the reaction proceeds through the conversion of $^{\bullet}O_3^-$ to •OH [13]. The lower reactivity of 1,4-dioxane with molecular O_3 at pH ≤ 7 results from the absence of significantly electron-rich sites in the molecular structure of 1,4-dioxane.

The pseudo-first-order kinetics constant was obtained from Equation (5), since the reactor was operated under an excess of ozone. The rate constants of 1,4-dioxane removal (k_1) at pH 3.0, 5.5 and 7.0 were quite similar (0.00061 ± 0.00007 min^{-1}, 0.00071 ± 0.00007 min^{-1}, 0.00065 ± 0.00004 min^{-1} respectively). In contrast, at

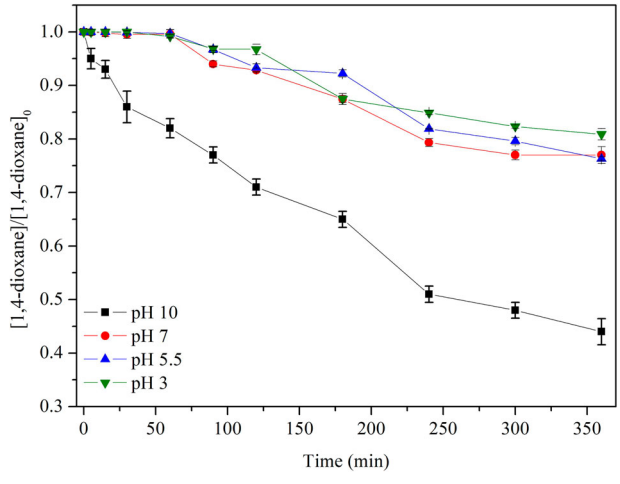

Figure 3. Kinetics of 1,4-dioxane removal at different pH values ([1,4-dioxane] = 200 ppm; ozone flow = 0.064 m^3 h^{-1}; $T = 25 \pm 1$°C).

pH 10 a significantly higher value was reached (0.00249 ± 0.00008 min^{-1}). Barndõk and collaborators [13] determined significantly higher pseudo-first-order rate constants for 1,4-dioxane degradation, under an excess of ozone, at pH 7.0 and 10.0 (1.2 and 30 min^{-1}, respectively). The faster kinetics may have resulted from the use of constant pH throughout the experiment and a significantly higher ozone flow rate (0.24 m^3 h^{-1}).

However, the rate constants for the decomposition of ozone over the CuO catalyst (k_{het}, Table 2) were at least 3 orders of magnitude higher than that for the reaction of ozone with 1,4-dioxane at pH 5.5 (0.00071 ± 0.00007 min^{-1}). As a consequence, in the presence of CuO, the degradation of 1,4-dioxane by direct ozonation alone is slow in comparison to the reaction between 1,4-dioxane and the free radicals produced by the ozone decomposition on the solid surface at pH 5.5.

Catalyzed ozonation of 1,4-dioxane with CuO

In heterogeneous catalytic ozonation, the role of the pH involves multiple aspects, including the decomposition of the ozone molecules, the surface properties of the catalyst and the charge of ionizable organic molecules, which in turn affects the production of reactive oxygen species (ROS) and the degradation rate of water contaminants [24,25]. The effect of the initial pH on 1,4-dioxane degradation and mineralization under catalytic ozonation was investigated using 250 ppm of CuO. The results in Figures S2a and S2b show that the rate of TOC and 1,4-dioxane removal increased slightly as the pH increased and the rate of degradation was considerably higher at pH 10. The relatively small impact of the initial pH observed in these unbuffered experiments can be attributed to the relatively fast decrease in the pH, which reached a plateau at similar pH values (around 5 to 6) (Figure S2c).

The concentration profiles for ozone in the aqueous phase observed during the experimental runs can be seen in Figure 4a. The concentration of ozone in the absence and in the presence of CuO rapidly increased during the initial stage of the reaction, reaching equilibrium concentrations (C_e) approaching the saturation values, observed in the absence of 1,4-dioxane at the temperature of the experiments (Table 2). These results demonstrate that the gas-liquid ozonation reactions occurred through a relatively slow kinetic regime (small Hatta numbers) [49].

The pseudo-first-order rate constants of ozonation and CuO catalytic ozonation of 1,4-dioxane as a function of pH are shown in Figure 4b (mineralization) and c (degradation). The k_1 value for catalytic ozonation at pH 7, with 250 ppm of CuO, increased by factors of

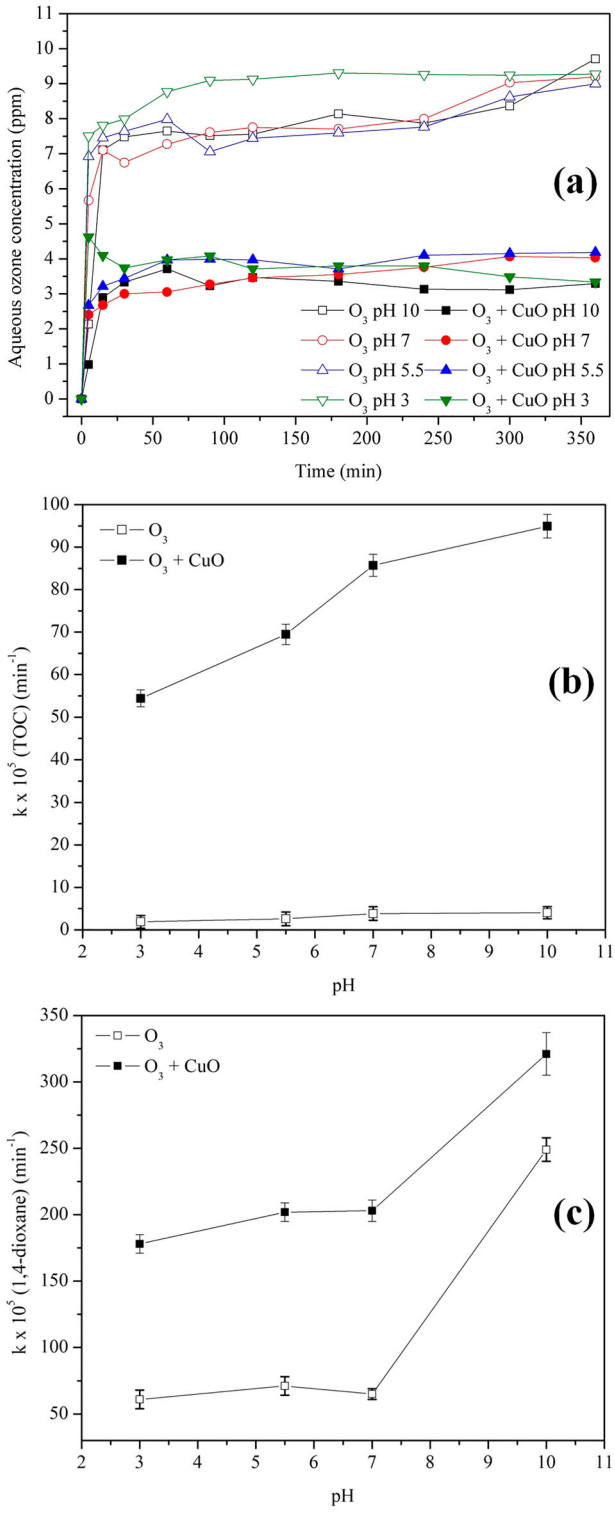

Figure 4. (a) Aqueous ozone concentration in the absence and presence of CuO, (b) pseudo-first order constants for 1,4-dioxane and (c) pseudo-first-order constants for TOC at different initial pH values during 1,4-dioxane catalytic ozonation ([CuO] = 250 ppm; [1,4-dioxane] = 200 ppm; ozone flow = 0.064 m^3 h^{-1}; T = 25 ± 1°C; t = 360 min).

22.3 and 3.12 for TOC and 1,4-dioxane removal, respectively, in comparison to ozonation. The increase in the

TOC removal with an initial pH of 10 is not significant, especially in the absence of CuO, due to the decrease in the pH during the reactions. It is known that the ozone decomposition with the formation of hydroxyl radicals is greatly enhanced under highly alkaline conditions [27]. However, the pH decreased during the reaction and reached a value of 4 after 6 h. The k_1 value at pH 3 increased by factors of 28.63 and 2.91 for TOC and 1,4-dioxane removal, respectively in comparison to ozonation. It is expected that homogeneous catalytic ozonation also could occur due to leaching of copper ions, that increased from 0.1%, 0.3% to 4.9% at the initial pH of 7.0, 5.5 and 3.0, respectively. Although the homogeneous catalytic ozonation cannot be neglected at the initial pH 3 due to copper leaching as Cu^{2+} ions, at pH circumneutral the main reactions responsible to 1,4-dioxane degradation occur as a heterogeneous catalytic process. Conversely, a significant impact on the rate of TOC and 1,4-dioxane removal (Figure S3) was observed as the concentration of CuO was increased from 100 to 3000 ppm, at neutral pH.

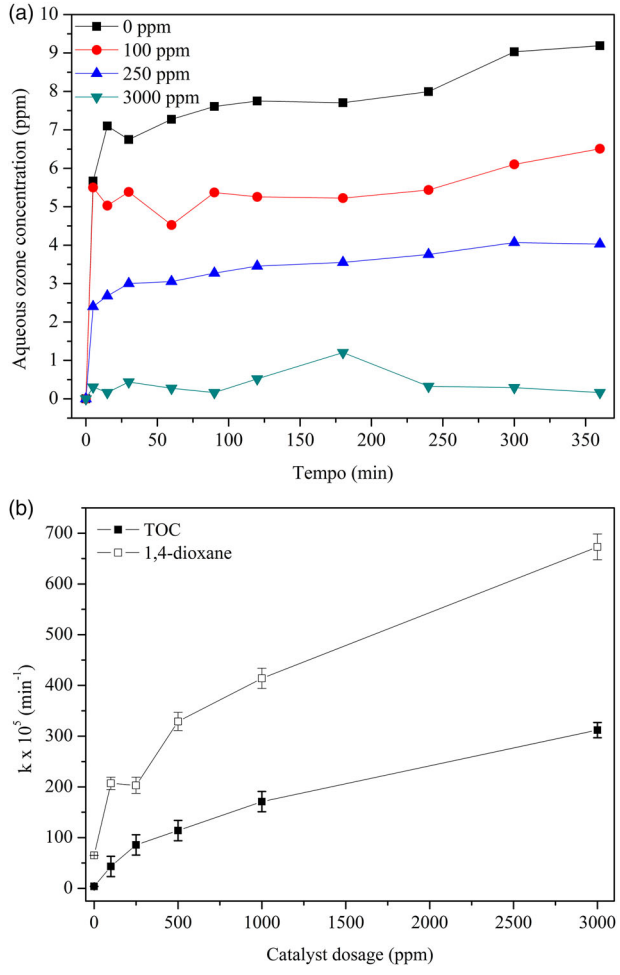

Figure 5. (a) Aqueous ozone concentrations with different catalyst dosages; (b) Pseudo-first-order constants for 1,4-dioxane and TOC removal after 6 h of reaction at different dosages of CuO ([1,4-dioxane] = 200 ppm; pH = 7.0 ± 0.5; ozone flow = 0.064 m^3 h^{-1}; T = 25 ± 1°C).

The pseudo-first-order kinetics constants at different catalyst concentrations are reported in Figure 5b. It can be observed that the rate constants (k_1) increased by factors of 81.25 and 10.35 for TOC and 1,4-dioxane removal, respectively, at pH 7 with 3000 ppm of CuO. These values suggest that 1,4-dioxane and TOC removal are strongly dependent on the amount of catalyst used, in agreement with results reported in the literature for other target water contaminants [20,26,50].

An increase in the catalyst surface area and the amount of active sites available favoured the decomposition of ozone, as shown by the lower equilibrium concentrations of ozone in solution (Figure 5a). The subsequent enhanced production of ROS and the reaction with 1,4-dioxane and its breakdown products led to higher rates of mineralization [20,50].

In the absence of ozone, 1,4-dioxane would be removed by adsorption onto the solid surface, because the formation of free radicals at room temperature is negligible [51]. In fact, CuO is an effective catalyst for the degradation of organic compounds by wet catalytic oxidation via a radical reaction mechanism [52], but these reactions only occur at high temperature (200–325°C) and pressure (5–15 MPa) in the presence of oxygen/air [53].

The impact of the adsorption of 1,4-dioxane by CuO can be considered negligible, since only 4% of the TOC and 8% of the 1,4-dioxane was adsorbed by 3000 ppm of CuO after 6 h (Figure S4). The low adsorption capacity of CuO is due to its low specific area (Table 1), the high solubility of 1,4-dioxane in water and low pressure, which also results in insignificant removal by adsorption on activated carbon [13].

The results collectively show that the effect of catalytic ozonation in the presence of CuO was higher than the combined effect of adsorption onto the catalyst surface and ozonation in the absence of catalyst, demonstrating that CuO is a highly active ozonation catalyst for the mineralization of 1,4-dioxane.

Radical species and reaction mechanism

The nature of the ROS produced during the CuO catalytic ozonation reaction was investigated in the presence of selected radical scavengers: salicylic acid (SA), sodium fluoride (NaF), 1,4-benzoquinone (PBQ) and phosphate (PHOS). The results in Figure 6 show the pseudo-first-order rate constant for the 1,4-dioxane and TOC removal. The TOC was evaluated for reactions with NaF

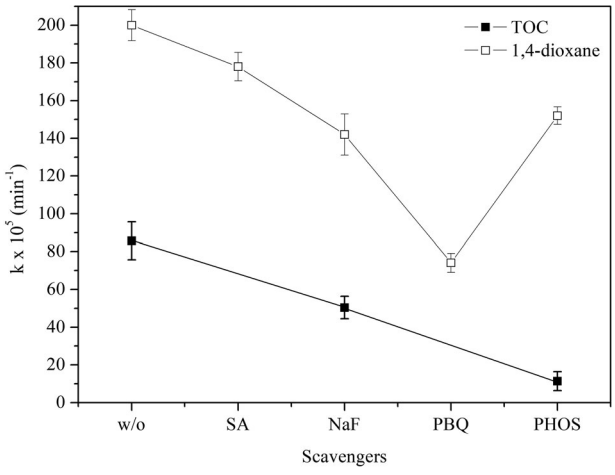

Figure 6. Pseudo-first-order constants for 1,4-dioxane and TOC removal after 6 h of reaction in the presence of selected radical scavengers ([1,4-dioxane] = 200 ppm; [CuO] = 250 ppm; pH = 7.0 ± 0.5; ozone flow = 0.064 $m^3\ h^{-1}$; T = 25 ± 1°C; [SA] and [PBQ] = 10 mM; [NaF] = 60 mM; [PHOS] = 40 mM).

and PHOS because these scavengers had no influence on the TOC detection.

SA and NaF were used to determine the role of $\cdot OH_{free}$ and $\cdot OH_{ads}$, respectively, in the degradation of 1,4-dioxane, [19,48]. Although *tert*-butanol (TBA) is generally used as an ·OH scavenger this was not employed in this study since the second-order reaction rate of TBA with ·OH ($5.0 \times 10^8\ M^{-1}\ s^{-1}$, [54]) was slower than the reaction rate of 1,4-dioxane with ·OH ((1.1 to $2.35) \times 10^9\ M^{-1}\ s^{-1}$, [55]). On the other hand, SA reacts faster with ·OH, with a reaction rate of $2.2 \times 10^{10}\ M^{-1}\ s^{-1}$ [56].

The reaction rate in the presence of SA decreased only slightly (by a factor of 1.2), indicating that $\cdot OH_{free}$ had a negligible effect on the 1,4-dioxane degradation. In the presence of NaF, the reaction rate decreased by factors of 1.4 and 1.7 for 1,4-dioxane and TOC, respectively, suggesting that $\cdot OH_{ads}$ had a stronger influence in the degradation of the intermediate products. In contrast, in the presence of PBQ, a superoxide radical ($O_2^{-\cdot}$) scavenger [57,58], the reaction rate decreased by a factor of 2.7, indicating that 1,4-dioxane was mainly degraded by $O_2^{-\cdot}$.

Lewis acid sites are considered to be catalytic centres on the catalyst surface for ozone decomposition reactions [32,59]. On the other hand, PHOS has high affinity toward the Lewis acids and thus can fill the active sites on the surface of catalysts, leading to a loss of catalytic activity. Figure 6 shows that in the presence of PHOS the reaction rate decreased by factors of 7.52 and 1.32 for TOC and 1,4-dioxane removal, respectively, suggesting that the adsorption of ozone on the catalyst surface was prevented. This effect was more significant for the degradation of the intermediate products compared with the removal of 1,4-dioxane.

The reaction intermediates detected by GC-MS in the experiment using 3000 ppm of CuO at pH 7 were investigated to elucidate further the degradation of 1,4-dioxane by ozone alone and by catalytic ozonation. Similar intermediates were detected in the two cases; however, the appearance of the primary intermediates was faster and more pronounced in the presence of CuO. Ethylene glycol, formic acid and succinic acid were identified as the major reaction intermediates and the evolution of their concentrations in the presence of CuO can be seen in Figure S5.

A simplified reaction scheme for 1,4-dioxane decomposition by catalytic ozonation with CuO is given in Figure 7. The presence of ethylene glycol (EG) and formic acid (FA) as reaction intermediates, suggested that the degradation pathway mainly progressed through the formation of ethylene glycol diformate (EGDF) [60,61], although this compound was not detected by GC-MS as it quickly hydrolyzes to EG [13] and FA [62]. It should be noted that EG has previously been reported as the main intermediate of 1,4-dioxane during ozonation [13], electrolysis/O_3 [63], Fenton [61] and UV/H_2O_2/Fe^0 [60] treatments.

Catalyst stability and reusability

The recyclability and stability of the catalyst are critical factors for the large-scale application of heterogeneous catalytic ozonation systems for water and wastewater treatment. In this study, the recyclability and stability of the CuO used in the treatment of 1,4-dioxane by catalyst ozonation were assessed during five consecutive reuse cycles.

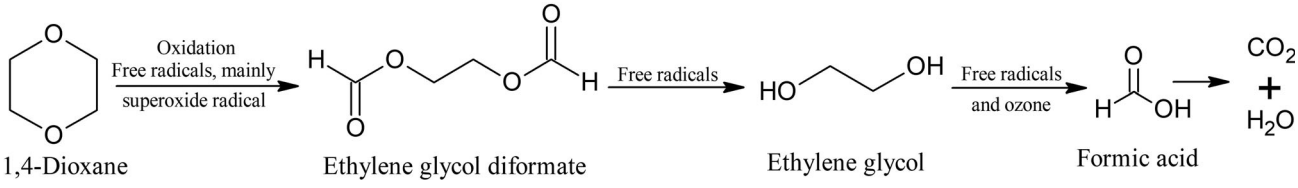

Figure 7. Simplified schematic of 1,4-dioxane decomposition by catalytic ozonation with CuO ([1,4-dioxane] = 200 ppm, [CuO] = 3000 ppm, pH = 7.0 ± 0.5, ozone flow = 0.064 $m^3\ h^{-1}$ and T = 25 ± 1°C).

The catalytic activity of CuO during each cycle decreased slightly (Figure 8a) but remained at acceptable values. The TOC and 1,4-dioxane removal efficiencies decreased from 49% to 30% and from 78% to 56%, respectively, but were still significantly higher than the removals achieved with ozonation alone (20% for 1,4-dioxane and negligible for TOC). The apparent loss of activity could result from the poisoning of the active sites, fouling of the catalyst surface by the reaction products, the loss of catalyst mass during each reusing cycle and copper leaching [20,21].

The FTIR spectra for the CuO before and after five cycles of catalytic ozonation (Figure 8b) show no alterations, suggesting good stability and structural composition of the catalyst. A strong absorption band peak

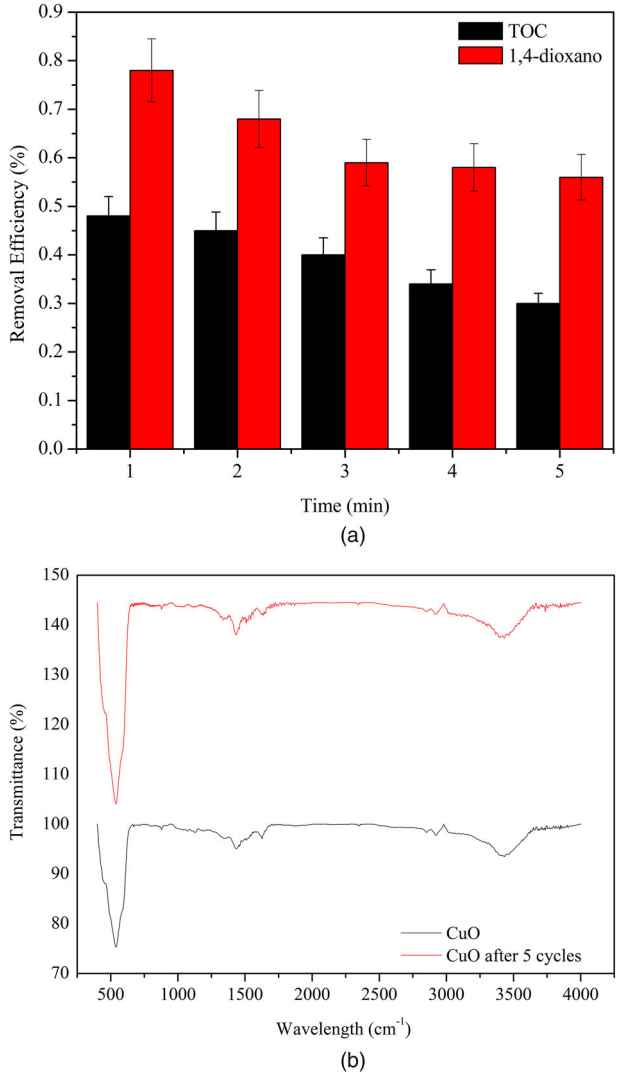

Figure 8. (a) The stability and reusability of CuO in the catalytic ozonation of 1,4-dioxane over 5 cycles and (b) FTIR spectra of CuO before and after 5 cycles of catalytic ozonation ([1,4-dioxane] = 200 ppm; pH = 7.0; ozone flow = 0.064 $m^3 h^{-1}$; T = 25 ± 1°C; [catalyst] = 1000 ppm; reaction time: 360 min).

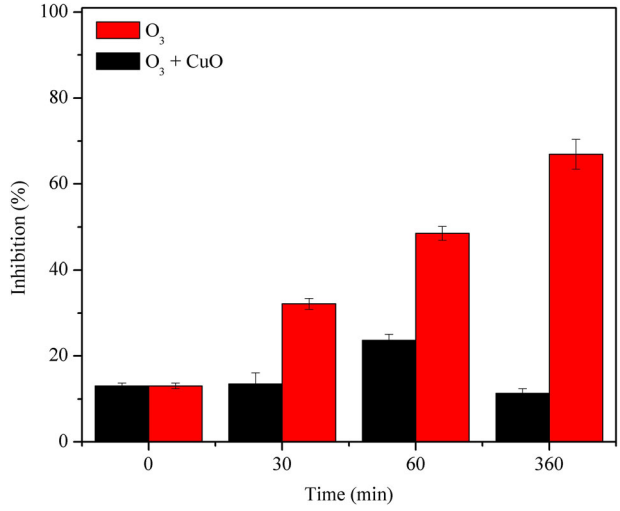

Figure 9. Acute toxicity of 1,4-dioxane and byproducts after ozonation or catalytic ozonation for 0, 30, 60 and 360 min ([1,4-dioxane] = 200 ppm; pH = 7.0; ozone flow = 0.064 $m^3 h^{-1}$; T = 25 ± 1°C; [catalyst] = 3000 ppm; reaction time: 360 min).

was observed at 539 cm^{-1} due to the vibrational stretching of CuO [61]. The peaks observed in the range of 1107 and 1637 cm^{-1} may be attributed to O-H bending vibrations combined with copper atoms. The presence of humid air and hydrated CuO samples was responsible for the formation of peaks in the range of 2900 and 3500 cm^{-1} [64].

Copper leaching from the catalyst to the solution during catalytic ozonation at pH 7 was quantified after each cycle by AAS. Copper leaching was 0.28, 0.26, 0.2, 0.12 and 0.7 ppm for cycles 1, 2, 3,4 and 5, respectively. The sum of the amount of copper dissolved in the aqueous media during all cycles was less than 0.1%, indicating that the CuO catalyst has a high degree of stability.

Acute toxicity test with Vibrio fischeri

The toxicity results for the water containing 1,4-dioxane, before and after treatment in the absence and presence of CuO (3000 ppm), after 0, 30, 60 and 360 min, are shown in Figure 9. The acute toxicity observed after the treatment in the presence of CuO was significantly lower than that observed after the treatment in the absence of the catalysis. Catalytic oxidation with CuO increased the mineralization rate of the toxic intermediates formed during the 1,4-dioxane oxidation treatment, as also observed in the case of treatment by the photo-electron-peroxone process [65]. Notably, the toxicity of the samples treated by ozonation alone increased significantly during the treatment process, presumably due to the insignificant rate of mineralization observed,

suggesting a gradual accumulation of toxic intermediates in solution, in agreement with the results obtained using the electro-peroxone process [15]. This observation indicates that detailed toxicity studies need to be performed before implementing advanced water treatment processes.

Conclusions

This study demonstrated the effective treatment of 1,4-dioxane by catalytic ozonation using CuO. It was found that the mechanism of reaction involves primarily superoxide radicals, rather than hydroxyl radicals. These in turn react with 1,4-dioxane to form ethylene glycol, which was further decomposed to formic acid with a higher rate of mineralization when compared with ozonation alone. This further contributed to reducing the acute toxicity of the treated water. In contrast, in the absence of catalyst the toxicity of the water increased after treatment by ozonation at circumneutral pH.

Disclosure statement

No potential conflict of interest was reported by the authors.

Funding

The authors would like to acknowledge CAPES/Brazil (Coordenação de Aperfeiçoamento de Pessoal de Nível Superior) for scholarships (grant number 0001), CNPq/Brazil (Conselho Nacional de Desenvolvimento Científico e Tecnológico) for financial support [grant number 405892/2013 6], LCME (Central Laboratory of Electronic Microscopy) for the MET analysis and Édipo Silva for zeta potential measurements. Partial funding was provided by the NSF Engineering Research Center on Nanotechnology - Enabled water treatment.

ORCID

Gidiane Scaratti http://orcid.org/0000-0002-1992-2916
Regina F. P. M. Moreira http://orcid.org/0000-0002-2863-7260

References

[1] Weimar R. Prevent groundwater contamination before it's too late. Water Wastes Eng. 1980;17:30–33.
[2] Abe A. Distribution of 1,4-dioxane in relation to possible sources in the water environment. Sci Total Environ. 1999;227(1):41–47.
[3] USEPA. Treatment technologies for 1,4-dioxane: fundamentals and field applications, EPA-542-R-06-009. Office of solid waste and emergency response. Washington (DC): USEPA; 2006.
[4] Mohr TKG. Environmental investigation and remediation: 1,4-dioxane and other solvent stabilizers. CRC Press; 2010.
[5] Barndõk H, Hermosilla D, Negro C, et al. Comparison and predesign cost assessment of different advanced oxidation processes for the treatment of 1,4-dioxane-containing wastewater from the chemical industry. ACS Sustain Chem Eng. 2018;6(5):5888–5894.
[6] ECB. E.U. risk assessment report: 1,4-dioxane, ISBN 92-894-1252-6, second priority list. Vol. 21. Luxembourg: Office for Official Publications of the European Communities; 2002. p. 1–129.
[7] USEPA. Toxicological review of 1,4-dioxane (CAS No. 123–91-1), EPA/635/R-09/005-F. Washington (DC): USEPA; 2010.
[8] Kim HS, Kwon BH, Yoa SJ, et al. Degradation of 1,4-dioxane by photo-Fenton processes. J Chem Eng Jpn. 2008;41:829–835.
[9] So MH, Han JS, Han TH, et al. Decomposition of 1,4-dioxane by photo-Fenton oxidation coupled with activated sludge in a polyester manufacturing process. Water Sci Technol. 2009;59:1003–1009.
[10] Li M, Mathieu J, Liu Y, et al. The abundance of tetrahydrofuran/dioxane monooxygenase genes (thmA/dxmA) and 1,4-dioxane degradation activity are significantly correlated at various impacted aquifers. ES&T Letters. 2014;1:122–127.
[11] Vescovi T, Coleman HM, Amal R. The effect of pH on UV-based advanced oxidation technologies-1,4-dioxane degradation. J Hazard Mater. 2010;182:75–79.
[12] Kiker JH, Connolly JB, Murray WA, et al. Ex-situ wellhead treatment of 1,4-dioxane using Fenton's reagent. Proc Annu Int Conf Soils, Sediments. Water Energy. 2010;15:210–226.
[13] Barndõk H, Cortijo L, Hermosilla D, et al. Removal of 1,4-dioxane from industrial wastewaters: routes of decomposition under different operational conditions to determine the ozone oxidation capacity. J Hazard Mat. 2014;280:340–347.
[14] Eberle D, Ball R, Boving TB. Peroxone activated persulfate treatment of 1,4-dioxane in the presence of chlorinated solvent co-contaminants. Chemosphere. 2016;144:728–735.
[15] Wang H, Bakheet B, Yuan S, et al. Kinetics and energy efficiency for the degradation of 1,4-dioxane by electro-peroxone process. J Hazard Mater. 2015;294:90–98.
[16] Adams CD, Scanlan PA, Secrist ND. Oxidation and biodegradability enhancement of 1,4-dioxane using hydrogen peroxide and ozone. Environ Sci Technol. 1994;28:1812–1818.
[17] Suh JH, Mohseni M. A study on the relationship between biodegradability enhancement and oxidation of 1,4-dioxane using ozone and hydrogen peroxide. Water Res. 2004;38:2596–2604.
[18] Chitra S, Paramasivan K, Cheralathan M. Degradation of 1,4-dioxane using advanced processes. Environ Sci Pollut Res. 2012;19:871–878.
[19] Kwon SC, Kim JY, Yoon SM, et al. Treatment characteristic of 1,4-dioxane by ozone-based advanced oxidation processes. J Ind Eng Chem. 2012;18:1951–1955.
[20] Ahmadi M, Kakavandi B, Jaafarzadeh N, et al. Catalytic ozonation of high saline petrochemical wastewater using PAC@FeIIFe$_2$IIIO$_4$: optimization, mechanisms and biodegradability studies. Sep Purif Technol. 2017;177:293–303.
[21] Vakilabadi DR, Hassani AH, Omrani G, et al. Catalytic potential of Cu/Mg/Al-chitosan for ozonation of real landfill leachate. Process Saf Environ. 2017;107:227–237.

[22] Sable SS, Ghute PP, Fakhrnasova D, et al. Catalytic ozonation of clofibric acid over copper-based catalysts: In situ ATR-IR studies. Appl Catal B- Environ. 2017;209:523–529.
[23] Ziylan-Yavaş A, Ince NH. Catalytic ozonation of paracetamol using commercial and Pt-supported nanocomposites of Al_2O_3: the impact of ultrasound. Ultrason Sonochem. 2018;40(B):175–182.
[24] Chen W, Li X, Pan Z, et al. Effective mineralization of diclofenac by catalytic ozonation using Fe-MCM-41 catalyst. Chem Eng J. 2016;304:594–601.
[25] Huang Y, Cui C, Zhang D, et al. Heterogeneous catalytic ozonation of dibutyl phthalate in aqueous solution in the presence of iron-loaded activated carbon. Chemosphere. 2015;119:295–301.
[26] Chen C, Chen H, Guo X, et al. Advanced ozone treatment of heavy oil refining wastewater by activated carbon supported iron oxide. J Ind Eng Chem. 2014;20:2782–2791.
[27] Zhang T, Li W, Croué J-P. A non-acid-assisted and non-hydroxyl-radical-related catalytic ozonation with ceria supported copper oxide in efficient oxalate degradation in water. Appl Catal B-Environ. 2012;121–122:88–94.
[28] Centurião APSL, Baldissarelli V, Scaratti G, de Amorim SM, Moreira RFPM. Enhanced ozonation degradation of petroleum refinery wastewater in the presence of oxide. Environ Technol. doi:10.1080/09593330.2017.1420103
[29] Tian GP, Wu QY, Li A, et al. Promoted ozonation for the decomposition of 1,4-dioxane by activated carbon. Water Sci Technol Water Supply. 2017;17(2):613–620.
[30] Zhang J, Huang G-Q, Liu C, et al. Synergistic effect of microbubbles and activated carbon on the ozonation treatment of synthetic dyeing wastewater. Sep Purif Technol. 2018;201:10–18.
[31] Xiong Z, Lai B, Yuan Y, et al. Degradation of p-nitrophenol (PNP) in aqueous solution by a micro-size Fe^0/O_3 process (mFe^0/O_3): optimization, kinetic, performance and mechanism. Chem Eng J. 2016;302:137–145.
[32] Kasprzyk-Hordern B, Ziólek M, Nawrocki J. Catalytic ozonation and methods of enhancing molecular ozone reactions in water treatment. Appl Catal B-Environ. 2003;46:639–669.
[33] Gharbani P, Mehrizad A. Heterogeneous catalytic ozonation process for removal of 4-chloro-2-nitrophenol from aqueous solutions. J Saudi Chem Soc. 2014;18:601–605.
[34] Hu E, Wu X, Shang S, et al. Catalytic ozonation of simulated textile dyeing wastewater using mesoporous carbon aerogel supported copper oxide catalyst. J Clean Prod. 2016;112:4710–4718.
[35] Von GU. Ozonation of drinking water: part I. Oxidation kinetics and product formation. Water Res. 2003;37:1443–1467.
[36] APHA. Standard methods for the examination of water and wastewater. 19th ed. Washington (DC): APHA; 1995.
[37] Scaratti G. Removal of 1,4-dioxane from industrial wastewaters: routes of decomposition using catalytic ozonation or peroxidation coupled to membrane filtration (qualifying exam – dissertation). Florianopolis: Federal University of Santa Catarina; 2017.
[38] Sullivan DE, Roth JA. Kinetics of ozone self-decomposition in aqueous solution. AlChe Symp Series. 1979;79:142–149.
[39] Li M, Conlon P, Fiorenza S, et al. Rapid analysis of 1,4-dioxane in groundwater by frozen micro-extraction with gas chromatography/mass spectrometry. Ground Water Monit R. 2011;31:70–76.
[40] ISO 11348-3. Water quality – determination of the inhibitory effect of water samples on the light emission of *Vibrio fischeri* (Luminescent bacteria test), part 3: method using freeze-dried bacteria. Geneva: International Organization for Standardization; 2007.
[41] Xu L, Srinivasakannan C, Peng J, et al. Synthesis of Cu-CuO nanocomposite in microreactor and its application to photocatalytic degradation. J Alloys Compd. 2017;695:263–269.
[42] Raj ASA, Biju V. Nanostructured CuO: facile synthesis, optical absorption and defect dependent electrical conductivity. Mat Sci Semicon. 2017;68:38–47.
[43] Ananth A, Dharaneedharan S, Heo M-S, et al. Copper oxide nanomaterials: synthesis, characterization and structure-specific antibacterial performance. Chem Eng J. 2015;262:179–188.
[44] Lupan O, Cretu V, Postica V, et al. Enhanced ethanol vapour sensing performances of copper oxide nanocrystals with mixed phases. Sensor Actuat B-Chem. 2016;224:434–448.
[45] Zhou L-J, Zou Y-C, Zhao J, et al. Facile synthesis of highly stable and porous CuO/CuO cubes with enhanced gas sensing properties. Sensor Actuat B-Chem. 2013;188:533–539.
[46] Shen Y, Guo M, Xia X, et al. Role of materials chemistry on the electrical/electronic properties of CuO thin films. Acta Mater. 2015;85:122–131.
[47] Huang L, Zheng M, Yu D, et al. In-situ fabrication and catalytic performance of Co-Mn@CuO core-shell nanowires on copper meshes/foams. Mater Des. 2018;147:182–190.
[48] Beltrán FJ. Ozone reaction kinetics for water and wastewater systems. 1st ed. Spain: Lewis Publishers; 2004.
[49] Lan BY, Nigmatullin R, Li Puma G. Ozonation kinetic of cork-processing water in a bubble column reactor. Water Res. 2008;42:2473–2482.
[50] Huang Y, Sun Y, Xu Z, et al. Removal of aqueous oxalic acid by heterogeneous catalytic ozonation with MnO/sewage sludge-derived activated carbon as catalysts. Sci Total Environ. 2017;575:50–57.
[51] Ji F, Li C, Deng L. Performance of CuO/oxone system: heterogeneous catalytic oxidation of phenol at ambient conditions. Chem Eng J. 2011;178:239–243.
[52] Sadana A, Katzer JR. Involvement of free radicals in the aqueous-phase catalytic oxidation of phenol over copper oxide. J Catal. 1974;35:140–152.
[53] Sushma KM, Saroha AK. Performance of various catalysts on treatment of refractory pollutants in industrial wastewater by catalytic wet air oxidation: A review. J Environ Manage. 2018;228:169–188.
[54] Hoigné J, Bader H. Rate constants of reactions of ozone with organic and inorganic compounds in water—II. Water Res. 1983;17:185–194.
[55] Thomas JK. Rates of reaction of the hydroxyl radical. Trans Faraday Soc. 1965;61:702–707.
[56] Crittenden JC, Trussel RR, Hand DW, et al. Water treatment: principles and design. John Wiley & Sons; 2012.
[57] Nawaz F, Xie Y, Cao H, et al. Catalytic ozonation of 4-nitrophenol over an mesoporous α-MnO with resistance to leaching. Catal Today. 2015;258:595–601.

[58] Yang M-Q, Zhang Y, Zhang N, et al. Visible-light-driven oxidation of primary C-H bonds over CdS with dual co-catalysts graphene and TiO_2. Sci Rep. 2013;3:3314.
[59] Mashayekh-Saehi A, Moussavi G, Yaghmaeian K. Preparation, characterization and catalytic activity of a novel mesoporous nanocrystalline MgO nanoparticle for ozonation of acetaminophen as an emerging water contaminant. Chem Eng J. 2017;310:157–169.
[60] Barndõk H, Blanco L, Hermosilla D, et al. Heterogeneous photo-Fenton processes using zero valent iron microspheres for the treatment of wastewaters contaminated with 1,4-dioxane. Chem Eng J. 2016;284:112–121.
[61] Merayo N, Hermosilla D, Cortijo L, et al. Optimization of the Fenton treatment of 1,4-dioxane and on-line FTIR monitoring of the reaction. J Hazard Mat. 2014;268:102–109.
[62] Vollhardt KPC, Schore NE. Organic chemistry: structure and function. 6th ed. W.H. Freeman and Co.; 2011.
[63] Kishimoto N. Dependeny of advanced oxidation performance on the contaminated water feed mode for ozonation combined with electrolysis using a two-compartment electrolytic flow-cell. J Adv Oxi Technol. 2015;10:241–246.
[64] Dubal DP, Dhawale DS, Salunkhe RR, et al. Fabrication of copper oxide multilayer nanosheets for supercapacitor application. J Alloys Compd. 2010;492:26–30.
[65] Shen W, Wang Y, Zhan J, et al. Kinetics and operational parameter for 1,4-dioxane degradation by the photoelectron-peroxone process. Chem Eng J. 2017;310:249–258.